Gas Bubble Entrainment by Plunging Laminar Liquid Jets

TONG JOE LIN and HAROLD G. DONNELLY

Wayne State University, Detroit, Michigan

A free, vertical jet of liquid plunging into a quiescent surface of the same liquid entrains the surrounding gas into the receiving liquid to form bubbles. The entrainment characteristics of such jets of Newtonian liquids of varying physical properties have been investigated by means of high-speed photography.

Although both laminar and turbulent jets entrain gas bubbles, the mechanisms governing the entrainment process of the two types of jets are clearly different. Entrainment by turbulent jets results from the disturbances on the free surface caused by the jet instability; entrainment by laminar jets is accomplished by the formation of a thin shell of gas around the jet at the point of entrance, by the development of oscillations in the shell, and by its subsequent break-up into bubbles.

Entrainment occurs only when the average jet velocity exceeds a certain critical value termed *minimum entrainment velocity*. For a laminar jet having a flat velocity profile at the point of entrance, the following correlation permits prediction of the minimum entrainment velocity:

$$\text{Weber number} = 10\ (\text{Reynolds number})^{0.74}$$

where the dimensionless numbers are based on the liquid properties and the jet diameter at the point where the jet meets the surface of the receiving liquid.

The falling of a liquid stream into the surface of an identical or different liquid often is accompanied by the formation of air bubbles. This is commonly observed during the pouring of a fluid into a container and in the formation of white water beneath waterfalls (*1*). Similar phenomena occurring in such industrial operations as the pouring of molten glass or polymer solutions create problems of concern to chemical engineers. In the paint, food, detergent, cosmetics, and pharmaceutical industries, bubbles of air entrained during filling operations of fluids through unsubmerged nozzles may escape readily or remain in the fluids for an indefinite time, depending chiefly on the bubble sizes and on the rheological properties of the fluids. The purpose of this work was to investigate the factors affecting the air entrainment process of a free, liquid jet plunging into a pool of the same liquid.

Although the literature concerned with the motion of air bubbles in liquids or the formation of bubbles in water by air blown through orifices is plentiful, the number of published reports concerned with the air entrainment process mentioned above is very small. In a somewhat related area, several workers have conducted studies of aeration involved in white water formation in rapids or spillways (*2* to *6*). However, the literature concerning the mechanism of air entrainment by plunging liquid jets is almost nonexistent. Shirley (*7*) and Ohyama, Takayama, and Idemura (*8*) performed some exploratory work in this area with mechanical, bubble-trapping devices, but in neither instance were liquids other than water used, nor was bubble entrainment observed when the jets were in laminar flow.

In the exploratory stages of the present work, the observation was made that smooth laminar jets also entrained air bubbles into the receiving liquid, but the entrainment was found to occur only when the jet velocity exceeded a certain critical value. High-speed motion pictures were then used to examine entrainment by both laminar and turbulent jets. The mechanism of laminar entrainment was seen to be quite different from that of turbulent entrainment. The study was then initiated to determine the effects on entrainment of the liquids' properties and of the jets' characteristics. Although both turbulent and laminar jets were studied, the principal investigation concerned gas entrainment by laminar jets.

EXPERIMENTAL

Apparatus

All bubble entrainment experiments were carried out in the 4-gal. transparent Plexiglas tank in the recirculation system shown in Figure 1. A centrifugal pump moved the fluid from the bottom of the tank to the circular discharge nozzles above the fluid surface to produce the vertical jets. By varying the nozzle size and the fluid circulation rate, the jet diameter and jet velocity could be adjusted to the desired values. In addition, the nozzle assembly was mounted on a vertical slide so that the jet length could be varied. Water sprayed on the pump casing removed the heat generated by the pump. An auxiliary cooler and an electric heater with a sensitive thermo-

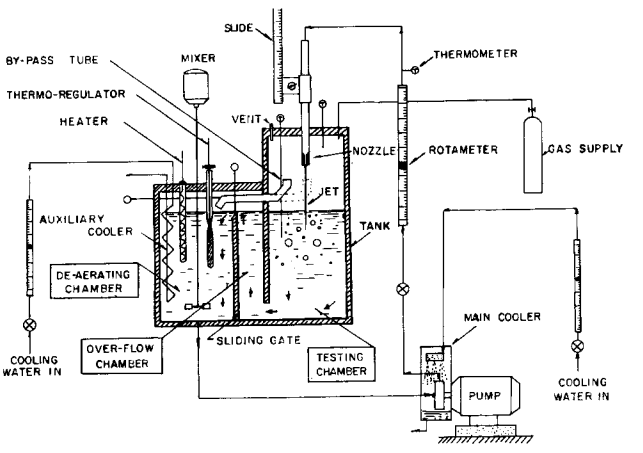

Fig. 1. Experimental apparatus.

Tong Joe Lin is with Max Factor and Company, Hollywood, California.

regulator were placed in the tank to adjust the fluid temperature to any desired level.

Tank Assembly. The fluid tank itself was divided into three sections: testing chamber, overflow chamber, and deaerating chamber. The jet of the fluid being tested was introduced to the testing chamber, where the entrainment process was observed or photographed. The fluid then passed into the overflow chamber through a slot at the bottom of the testing chamber, and subsequently was forced over a movable weir into the deaerating chamber. A movable by-pass tube diverted the flow from the jet nozzle directly to the deaerating chamber in order to have the testing chamber liquid free from bubbles before initiating every run.

Nozzles. The nozzles were made by forcing brass tubes onto cone-shaped shafts carefully machined to produce smooth contours. The diameters of the bell-mouth nozzle entrance were all 16 mm. and the exit diameters were 4.01, 6.01, and 8.1 mm. The vertical length of the tapered section of the nozzle was 20 mm. and the straight section was 2.5 times that of the exit diameter. The curvature of the vertical cross section of the tapered section of the nozzle was a quarter of an ellipse. The inner surface of each nozzle was carefully polished and coated with paraffin wax to assure a smooth surface. The outer surface of each nozzle was machined to fit tightly into a 16-mm. I.D. Plexiglas pipe. For producing jets of larger diameter, a 15-mm. I.D. glass tube with carefully ground ends was used in place of a nozzle.

Photographic Equipment. A high-speed Fastax WF-3 motion picture camera of the rotating-prism type permitted pictures to be taken at rates up to 8,000 frames/sec. The speed of the electric motor in the camera could be varied with a voltage control unit to produce time magnification from 9 to 500 times. By means of a solenoid attached to the by-pass tube of the testing chamber, the control unit provided the necessary synchronization of the camera and the experimental event. For the measurement of bubble size distribution, a 4 × 5 Graphic camera with Polaroid film holder was used in conjunction with the motion picture camera.

Testing Fluids. Although water and mineral oil were employed for some runs, aqueous solutions of U.S.P. grade glycerol, with viscosities from 10 to 400 centipoises were used in most instances for entrainment experiments. To study the effect of a surface-active agent, Tween-20 was added to some solutions. Since the concentrated glycerol solutions were highly hygroscopic, frequent determination of the viscosity was necessary to make certain that the solution did not absorb appreciable amounts of water from the air during the experiment.

Experimental Procedure

Before starting an experimental run, sufficient time was allowed for all bubbles in the tank to escape. To determine the minimum entrainment velocity for a given nozzle, the liquid was first circulated with the nozzle submerged beneath the liquid level in the testing chamber. The flow rates of the cooler were adjusted to maintain the temperature at 25°C. After all the air was purged from the line, the control valve was adjusted to set the jet flow rate slightly below the minimum required to entrain air. By maintaining the flow at this rate, the nozzle assembly was lifted slowly to set the nozzle at the desired height above the liquid surface. The jet flow rate was then gradually increased until bubbles were observed. From the flow rate and the jet diameter at the plunging point (that is, the point at which the jet enters the receiving fluid), the minimum entrainment velocity* was calculated.

Although this procedure was used to obtain the photographic data at the minimum entrainment velocity, a slightly different procedure was required to obtain the data at velocities above the minimum entrainment velocity. In these cases, the by-pass tube was used to prevent gas entrainment before the time of observation by diverting the jet fluid to the overflow chamber. After the flow was adjusted to the desired level and steady state was reached, the tube was pulled to the left, manually or electrically, to initiate gas bubble entrainment in the testing chamber. The motion pictures were then taken with camera speeds of from 1,000 to 7,000 frames/sec., depending on the rate of bubble formation. Still pictures were taken as desired immediately afterward.

Analysis of Data

The bubble diameter distributions were obtained by measuring the bubble images in photographic prints with a Brinell microscope. Where there was a sufficient number of bubbles in the photograph, fifty bubbles in focus were randomly selected for analysis. The frequency of bubble formation was determined from the analysis of the motion picture films with a variable speed projector equipped with a frame counter. The number of bubbles formed for a given interval was obtained by counting the bubble images on the screen. The exact time interval was determined from the time-light markings on the film.

To calculate the entrainment velocity, the diameter of the jet at the plunging point had to be accurately known. Due to gravitational acceleration, this diameter decreases with the distance from the nozzle. Precise calculation of the jet diameter as a function of the distance from the nozzle is extremely difficult, since the jet can expand or contract at the nozzle exit due to the development of normal stress (*9* to *11*). For this reason, actual measurements were made from the photographs of jet profiles for each system over a range of velocities.

Experimental Scope

The experiments covered twelve Newtonian liquids with viscosities ranging from 0.9 to 400 centipoises, with surface tensions varying from 30 to 63 dynes/cm., and with densities ranging from 0.876 to 1.246 g./cc. In most cases, the entrained gas was air at ambient conditions, but carbon dioxide at atmospheric pressure was substituted in several runs to determine the influence of gas properties. The temperature of the fluid was kept at 25 ± 1°C., although no attempt was made to regulate either the temperature or the humidity of air. The jet diameter at the plunging point varied from 2 to 12 mm. and the jet flow rates varied from about 5 to 120 cc./sec.

Experimental Code

In order to simplify the presentation, a code was assigned to each experimental system to identify the testing liquid, the entrained gas, and the nozzle size. The first number in the code represents the nominal nozzle diameter in millimeters. The letter or letters following this number indicate the liquid tested: *G* for glycerol solutions, *M* for mineral oil, H_2O for the water system. The presence of surfactant is identified by the use of primes. *G'*, *G''*, *G'''* indicate, respectively, the presence of 0.02%, 0.2%, and 0.3% surfactant in the glycerol solution. The number after this letter is the approximate vis-

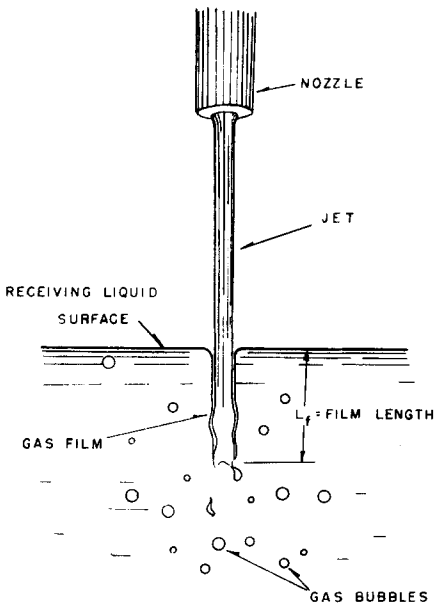

Fig. 2. Illustration of gas film below plunging point.

* Minimum entrainment velocity is defined as the minimum jet velocity, based on the jet diameter at plunging point, required to entrain bubbles in a given system.

cosity of the liquid at 25°C. Finally, a letter is employed to designate the gas surrounding the liquid jet; air is indicated by A and carbon dioxide by C.

For example, the system with code 6G200A means that air was entrained by jets of an aqueous glycerol solution having a viscosity of approximately 200 centipoises and discharging from a nozzle of approximately 6 mm. I.D. The only exception is a system designated by 8G400/300A. In this series, an aqueous glycerol solution of approximately 400 centipoises at 25°C. was used, but the temperature of the system was elevated so that the actual viscosity during the experimental run was approximately 300 centipoises.

RESULT AND DISCUSSION

The jet diameter variation with the jet length was determined from photographic profiles of jets. Analysis of high-speed motion picture films revealed the existence of a continuous, thin shell of gas beneath the plunging point during the entrainment process. This is illustrated in Figure 2. For a given system at a given flow rate, the length of the gas film fluctuated somewhat with time, but it appeared to maintain a fairly constant length. This equilibrium gas film length L_f was measured along with the size and frequency of formation of the bubbles. By assuming that all bubbles were spherical, an estimate of the volumetric rate of gas entrainment P was calculated from the frequency and size distribution data. A dimensionless P/Q ratio, the ratio of gas entrainment rate to liquid flow rate, was also calculated for each set of data. The complete tabulation of the data for all jet profiles, minimum entrainment velocities, bubble size distributions, bubble frequencies, equilibrium film lengths, and gas entrainment rates, as well as the detailed information on fluid properties, are available in reference *12*. The main results, their significance, and the correlation of data are discussed here, along with examples of the points under consideration.

Minimum Entrainment Velocity

Over two hundred runs were made in the determination of the minimum entrainment velocities of twenty-seven different systems. Most of the data were obtained in the laminar flow region, although a number of runs were made in the transition and turbulent regions. While examination of the data shows that a definite discontinuity exists at the transition region corresponding to a Reynolds number of approximately 1,500, the critical point corresponding to the minimum entrainment velocity is very distinct for all laminar flow runs, and most of the data are consistent and highly reproducible. A general discussion is presented below of the experimental results of the several variables affecting the minimum entrainment velocity, and of their correlation.

Effect of Jet Diameter, Nozzle Diameter, and Jet Length. Any change in jet diameter, nozzle diameter, and jet length was found to affect significantly the minimum entrainment velocity. However, since the nozzle size and the distance from the nozzle affected the jet diameters at a given point, it was necessary to determine whether these factors are independent or interrelated. A close examination of the minimum entrainment velocity data for a 400-centipoise glycerol solution showed that the effects of nozzle diameter and jet length were significant only in that they affected the jet diameter at the plunging point. This can be clearly seen from Figure 3, in which the minimum entrainment velocity V_e determined with three different nozzles is plotted against the jet diameter at the plunging point D_p. In spite of the fact that these data were obtained with widely different nozzle diameters and jet lengths, they form a continuous curve.

The same conclusion is reached by examination of the data for liquids of other viscosities flowing from nozzles ranging in size from 4.01 to 15.52 mm. It should be noted, however, that this conclusion applies only where the jet velocity distributions at the plunging point are uniform and where the flows of the jets are laminar.

The design at the nozzle entrance also appears to be insignificant in laminar jet entrainment, since the data obtained from a straight glass pipe fit well with those obtained from the formed brass nozzles.

For gas entrainment by jets having Reynolds numbers beyond 2,000, the effects of jet diameter and plunging height were significantly different from those obtained during laminar flow. For these cases, the volumetric flow rate at the minimum entrainment velocity Q_e is generally independent of the jet length Z and dependent only on the nozzle diameter. This implies entrainment will take place at any Z for a given Q_e, regardless of the magnitude of D_p. No surrounding shell of gas was formed at the minimum entrainment point in this region. The results suggest that the gas entrainment at high Reynolds numbers may be due to the surface irregularities produced as the result of jet instability. Since such an irregularity is nearly independent of Z, it would explain why Q_e is unaffected by Z.

Effect of Liquid Viscosity. As shown in Figure 4, the viscosity of the liquid plays a very significant role in the entrainment process. In this example, the data obtained with a series of glycerol solutions at $D_p = 6.5$ mm. show that the increase in viscosity from 100 to 300 centipoises reduces the magnitude of the minimum entrainment velocity to about one-half of the original value. It will also

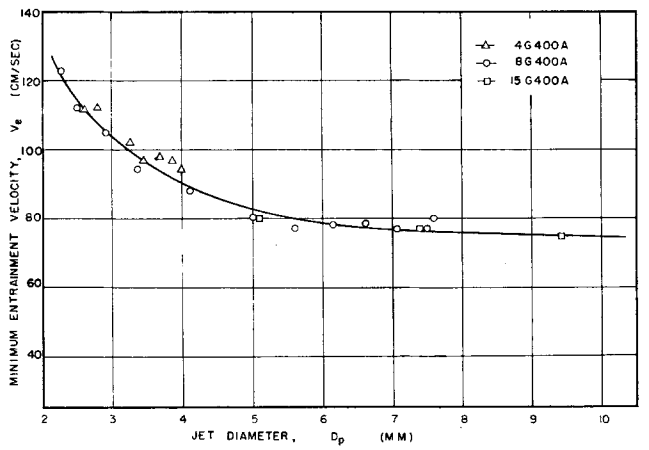

Fig. 3. Effect of jet diameter on minimum entrainment velocity.

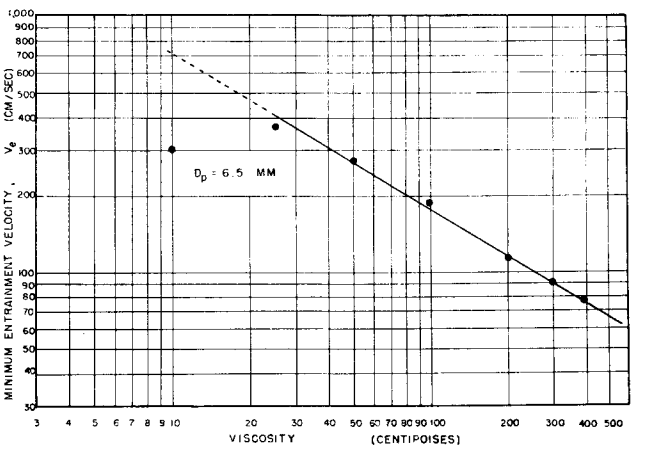

Fig. 4. Effect of viscosity on minimum entrainment velocity.

be noted that a discontinuity of data occurs at a point between 25 and 10 centipoises. The Reynolds numbers, based on the plunging point corresponding to these two values, are approximately 1,200 and 2,400, respectively. This suggests that different mechanisms govern the entrainment process in the low and high Reynolds number regions.

The above values were obtained with solutions having different viscosities but roughly constant density and surface tension. The data for the mineral oil runs, for which the surface tension and density are appreciably different from glycerol solutions, do not lie on the same curve. This indicates that the effects of surface tension and density also may be significant.

Effect of Surface-Active Agent. Figure 5 shows that the addition of a small quantity of surfactant has a marked effect in reducing the minimum entrainment velocity. The lowering of the minimum entrainment velocity appears to be parallel with the lowering of the solution surface tension. The surface tensions of the glycerol solutions shown are 59 dynes/cm. for 0% surfactant, 45 dynes/cm. for 0.02% surfactant solution, and 36 dynes/cm. for solutions containing 0.2% and 0.3% surfactant. Clearly, the presence of surfactant beyond 0.2% in this system produced a negligible effect on the surface tension or on the minimum entrainment velocity.

Effect of Jet Velocity Profile. As already stated, nozzle diameter and plunging height do not generally affect the minimum entrainment velocity except as they influence D_p. The data indicate that V_e decreases slightly with increase in D_p, as shown in Figures 3 and 5. However, deviation from this was observed when relatively low viscosity solutions were tested, using a portion of the jet close to the nozzle. For example, with 100-centipoise glycerol solutions (tested at values of Z from 1 to 17 cm. with an 8-mm. nozzle), the minimum entrainment velocity first decreased and then increased sharply with D_p. This is shown by the dotted line in Figure 6 (8G100A).

This peculiar effect seems significant only at Z values corresponding to short distances from the nozzle, since the data for large Z values are consistent with the data from the 4-mm. nozzle (4G100A) and the 15-mm nozzle (15G100A). Thus, if one disregards the data obtained for 8G100A from Z = 1 cm. to Z = 6 cm., a curve (shown as the solid line) in Figure 6 is obtained which lies parallel to those of other systems. Therefore, it appears that the deviation shown by the dotted line may be due to some jet characteristics prevailing only within a short distance from the nozzle tip.

This deviation is quite probably the result of a nonuniform velocity profile near the nozzle. Since complete relaxation of the velocity profile requires a finite time, the velocity of the jet surface, a short distance from the nozzle, must be less than the average velocity over the cross-sectional area. In such a nonuniform velocity profile region, the observed minimum entrainment velocity (which in this research is based on an average over the jet cross section) must exceed the normally expected value to produce a skin velocity equal to that which entrains gas.

In order to confirm the validity of this argument, a precise knowledge of velocity profile relaxation rate is required. Although a rigorous calculation of this relaxation rate is not available, an approximate solution based on the work of Hansen, Purchase, Wallace, and Woody (*13*) furnishes a semiquantitative basis for judgment.

By using the method of Hansen et al., the calculation for Z = 1 cm. in the 8G100A series shows that the ratio of surface velocity to average velocity $V_s/\overline{V}$ at the entrainment point was about 0.75; for Z = 7 cm., this ratio increased to 0.99, corresponding to a nearly flat velocity profile. The calculation thus seems to provide an explanation for the sudden increase of V_e for values of Z below 6 cm. in this example. Calculations for solutions with higher viscosities show the $V_s/\overline{V}$ ratio rapidly approaches unity at the minimum entrainment velocities observed. For example, the ratios at corresponding V_e values, for the 8G300A series are 0.98 and 0.99 at Z = 1 cm. and Z = 2 cm., respectively. This also explains why deviations from the curves were not observed in the 8G300A series, since all data taken were for values of Z greater than 1 cm.

Effect of Gas Properties and Other Factors. To investigate the effect of gas properties, carbon dioxide was introduced into the tank as the surrounding gas in several experimental runs. Comparison of data for the control runs with air and with carbon dioxide suggests that the effect of gas properties is probably negligible.

The effect of the fluid temperature was studied by raising the temperature of the fluid in the tank from 25° to 28.7°C. Examination of the data shows, however, that the influence of the temperature rise was equivalent to the effect gained by lowering the viscosity an amount corresponding to the temperature change. Thus, the effect of moderate temperature changes on minimum entrainment velocity is important only as it affects the fluid viscosity.

Correlation of Minimum Entrainment Velocity. To summarize the foregoing discussion, the factors clearly affecting minimum entrainment velocity are: liquid viscosity μ, liquid surface tension γ, and jet diameter at the plunging point D_p. The properties of the gas appear to have negligible effect, and the effect of temperature seems to be important only insofar as it affects the liquid viscosity. The effect of nozzle diameter is reflected only in the change

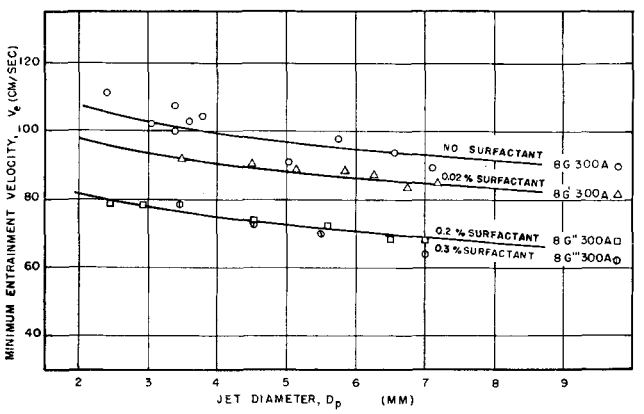

Fig. 5. Effect of surfactant on minimum entrainment velocity.

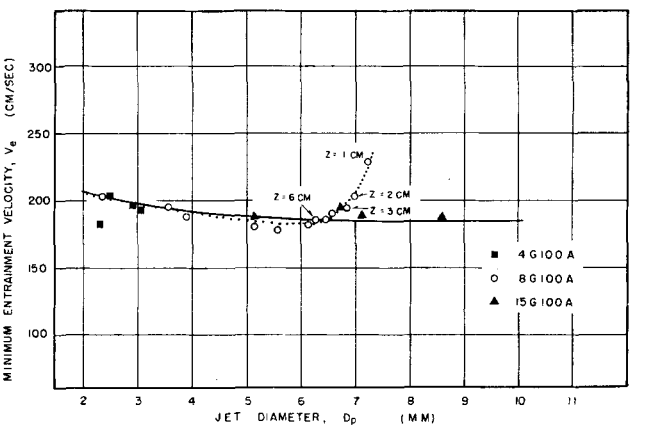

Fig. 6. Effect of velocity profile on minimum entrainment velocity.

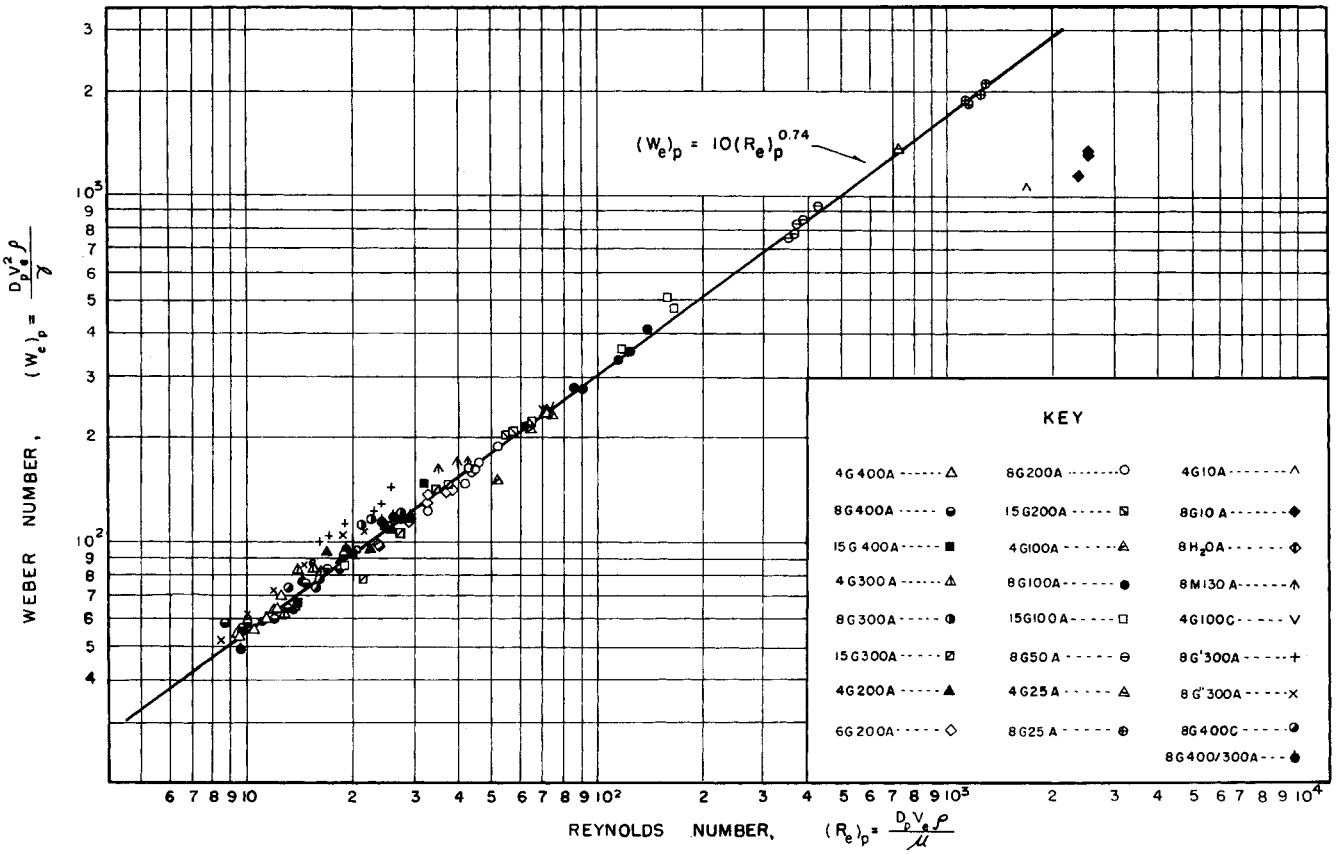

Fig. 7. Minimum entrainment velocity correlation.

of D_p. The jet length Z has importance only within the range where the velocity profile at the plunging point is nonuniform. Beyond such relaxation length of the jet, the effect of Z is essentially to change D_p. Although the effect of liquid density was not studied, this effect is regarded intuitively to be significant. Collectively, then, in the case of gas entrainment with a laminar jet having a flat velocity profile at the plunging point under atmospheric pressure, the present study suggests that the minimum entrainment velocity may be related to the following variables:

$$V_e = f(\mu, \gamma, \rho, D_p)$$

Using dimensional analysis, one obtains the following relation:

$$\left[\frac{D_p V_e^2 \rho}{\gamma}\right] = f\left[\frac{D_p V_e \rho}{\mu}\right]$$

The dimensionless group on the left-hand side of this equation is the Weber number, and the one on the right-hand side is the Reynolds number, both based on the variables at the plunging point.

Good correlation of the minimum entrainment velocity data was obtained when the Reynolds number was plotted against the corresponding Weber number at the plunging point. As shown in a log-log plot of Figure 7, all data fall within a narrow region of a straight line up to a Reynolds number of approximately 1,500. From the slope and the intercept of the line drawn through the data, the following empirical equation was obtained:

$$N_{We_p} = 10(N_{Re_p})^{0.74}$$

The groups N_{We_p} and N_{Re_p} represent the Weber number and the Reynolds number based on the jet diameter at the plunging point. The above relation holds well for all nozzle sizes used and for all liquid viscosities above 25 centipoises. The data for a mineral oil with physical properties considerably different from the glycerol series also fit the correlation quite well. As expected, considerable deviation occurs when the calculated surface velocity of the jet at the plunging point differs appreciably from the jet core velocity.

Although for most of the data the small deviations from the above equation appear to be solely the result of statistical error, some systematic deviations were observed in the surfactant series of studies. In the 8G′300 and 8G″300 series, in which the surfactant was added to reduce the surface tension, the data obtained lie consistently above the straight line of Figure 7. These deviations may, however, result from the failure to provide the necessary time for the solution containing surface-active material to reach surface equilibrium. In the present study, the surface of the jet and the receiving fluid were constantly renewed during any experimental run. Hence, if a finite time is required for a freshly formed surface to attain surface equilibrium, the surface tension during the entrainment experiment would be somewhat higher than the equilibrium surface tension measured by a duNoüy tensiometer. This would tend to make the Weber number higher than the actual value under the dynamic condition, since the value of surface tension used in calculating the Weber number is the equilibrium value.

The correlation developed from the data demonstrates the effect of liquid density on the minimum entrainment velocity, although that property of liquids was not specifically studied. By solving the equation for V_e the following relationship is obtained:

$$V_e = 6.22 \frac{\gamma^{0.794}}{D_p^{0.206} \rho^{0.206} \mu^{0.587}}$$

This relation clearly shows the minimum entrainment velocity decreases with increasing liquid density; likewise it provides an explanation for the low values of V_e observed in the mineral oil series in comparison with the glycerol series. The deviations were chiefly the result of

the low surface tension of the mineral oil rather than its lower density.

Overall, the correlation appears to be good in the laminar region. At Reynolds numbers exceeding 1,500, however, the correlation is no longer adequate and high-speed photography also reveals a change in entrainment mechanism.

Bubble Size and Frequency

Bubble size and the frequencies of bubble formation were determined at and above minimum entrainment velocities of the various systems studied. For simplicity the jet velocities were expressed in terms of a dimensionless entrainment velocity ratio α, defined as the ratio of the jet velocity at the plunging point to the corresponding minimum entrainment velocity. Data were obtained for values of α ranging from 1 to 2.1. The bubble formation rate at values of α larger than 2.1 was so great that accurate determination of bubble frequency was not feasible. This was particularly true in the experiments with low viscosity liquids, for which the minimum entrainment velocities were very high. For the range of experiments conducted, most of the bubbles observed had sizes varying from 0.5 to 3 mm., and the frequencies varied from 0.5 to over 2,000 bubbles/sec.

The dominant factor affecting both bubble size and bubble frequency was found to be the jet velocity during the entrainment process. Figures 8 and 9 show that the average bubble size decreases and the bubble frequency increases sharply with increase in jet velocity above the minimum entrainment velocity (that is, $\alpha = 1$).

The jet diameter at the plunging point D_p also affects the bubble size and frequency, although to a much more limited extent than does the rate of flow. Figures 10 and 11 indicate an increase in both bubble size and frequency over a two- to threefold increase in jet diameter, with the size of the bubbles being less significantly affected than the frequency. In fact, Figure 10 exaggerates the influence of D_p on bubble size, since the minimum entrainment velocity itself decreases with increasing D_p, and therefore provides somewhat larger bubbles in conformance with the relationships shown in Figure 8. On the other hand, the exponential rise in bubble frequency with increasing D_p, as shown in Figure 11, indicates the jet diameter at the plunging point to have a much more significant influence on bubble frequency than does the relatively small decrease in velocity resulting from the increase in D_p.

Figures 10 and 11 also illustrate the effect of the presence of a surface-active agent on the size and frequency of entrained bubbles. The addition of 0.02% of Tween-20 to the 300-centipoise glycerol solution, not only reduced

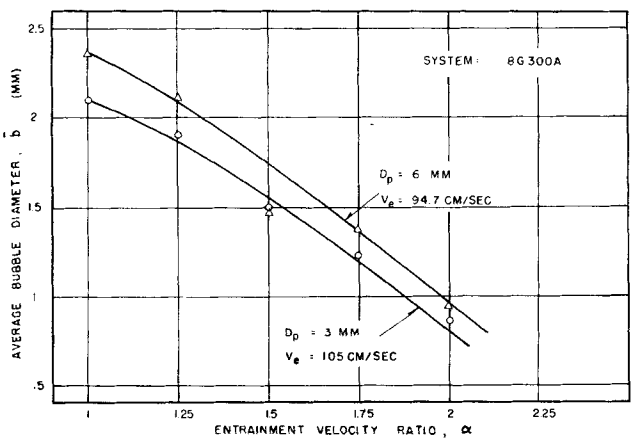

Fig. 8. Effect of jet velocity on average bubble diameter.

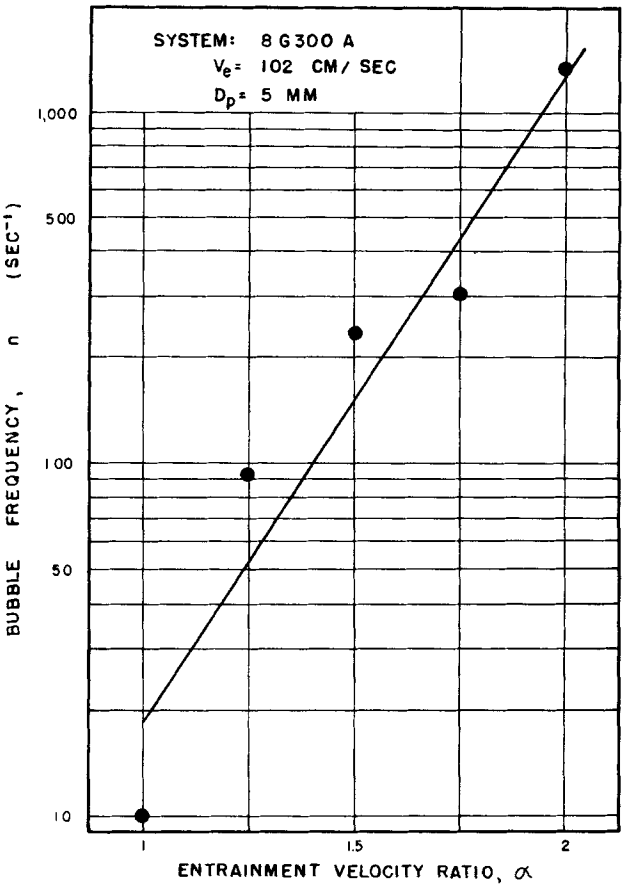

Fig. 9. Effect of jet velocity on bubble frequency.

the surface tension from 59 to 45 dynes/cm., but also reduced the average diameter and increased the frequency of formation of the bubbles produced from each nozzle at the minimum entrainment conditions for the particular system. The magnitudes of these effects are appreciably larger than is apparent in the figures, since the addition of the surfactant lowers the minimum entrainment velocity (see Figure 5). Since the lowered minimum entrainment velocity favors both an increase in bubble diameter and a decrease in frequency of bubble formation, the spread between the curves of Figures 10 and 11 would be even greater if the comparison were made at the same velocities.

The properties of the entrained gas appeared to have no effect on either bubble size distribution or bubble frequency. Within the range of experimental error, the data obtained with carbon dioxide proved to be no different from the data taken with air at atmospheric pressure.

Unlike minimum entrainment velocity, the reproducibility of the bubble size distribution and frequency data were only fair. The small sample size, the difficulty in counting and measuring very small bubbles, and the viscosity variation caused by minor temperature variation or from the slight change in moisture content of glycerol solution were probable sources of error in this phase of the research.

Rate of Gas Entrainment

Although it is clear from Figures 8 and 9 that the bubble frequency increases rapidly and the bubble size decreases sharply as the flow rate of the jet increases from the minimum entrainment velocity, it is of interest to determine how the volumetric rate of air entrainment in cc./sec. P varies with the liquid flow rate Q. To that end a measure of the entrainment rate for each experimental

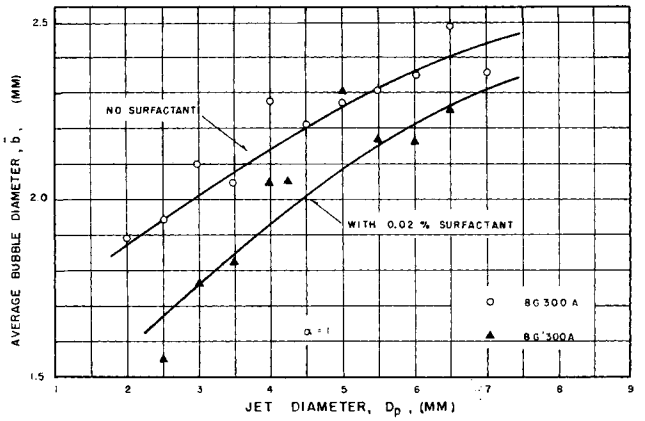

Fig. 10. Effect of surfactant on bubble size (at minimum entrainment velocities).

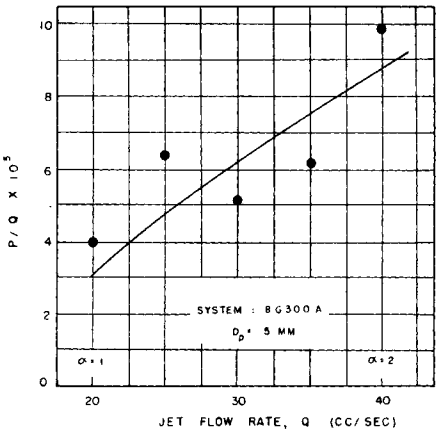

Fig. 12. Effect of jet flow rate on P/Q ratio.

run was calculated indirectly from the bubble size distribution and frequency data by assuming all bubbles were spherical. The calculation shows that while P increases markedly with Q, the increase of the P/Q ratio with Q is relatively moderate. Figure 12 shows a plot of P/Q vs. Q for a series of runs at a constant jet diameter. In this example, the increase of α from one to two caused increases in the frequency from 10 to 1,340 bubbles/sec. and in the volumetric entrainment rate P from 0.08 to 0.39 cc./sec. The P/Q ratio, however, increased from 4 $\times$ 10^{-3} to only 9.9 $\times$ 10^{-3}. The average bubble size dropped from 2.3 to 0.7 mm.

Examination of other sets of data also showed that, in spite of the large variation in bubble frequency, the P/Q ratios remained fairly constant. Furthermore, it was found that nearly 80% of the data obtained in the laminar region had values of P/Q ratio between 3 $\times$ 10^{-3} to 10 $\times$ 10^{-3}.

Entrainment Mechanism

Observations throughout this investigation show the entrainment of gas bubbles by a laminar jet is caused by the breakup of the gas film formed at the plunging point (see Figure 13, taken from below the liquid surface). Full comprehension of the bubble entrainment process requires clear understanding of the nature of the gas film and the mechanism of its breakup. During the analysis of the high-speed motion pictures of several runs, the thickness of this film was estimated from the projected image by measuring both the length of the piece of film broken away from the main film shell and the diameter of the bubble or bubbles subsequently formed. By this method, the estimated value of the film thickness is of the order of 1 to 5 $\times$ 10^{-3} cm.

The equilibrium average length of the gas film varied from 0 to 4.5 mm., depending on the system. In general, a viscous jet at low velocity favors the formation of long gas-film shells. It was observed that the upper portion of a long gas film generally remained cylindrical in shape, but the lower portion oscillated constantly as indicated by the photographs in Figure 14. The oscillations were roughly symmetrical in axial direction; they were slow at low velocity, but very rapid in the high flow rate runs. It is known that the instability of a liquid jet into a second liquid results in breakup of the jet into droplets (*14*). It is quite probable that, in the process of air entrainment by a laminar jet, the air film that separates the jet from the surrounding liqud produces a system much like the flow of a jet into a liquid of different properties. The breakup of the liquid jet would then naturally cause detachment of the gas film shell. The photographs shown also suggest that the process may be similar to a varicose breakup, where the jet is pinched off at the tip due to the growth of symmetrical disturbances.

Analysis of the high-speed motion pictures, as well as the discontinuity of the data in the transition region, indicates that the mechanism involved in gas entrainment by jets at high Reynolds numbers significantly differs from that of laminar jets. No surrounding gas film was

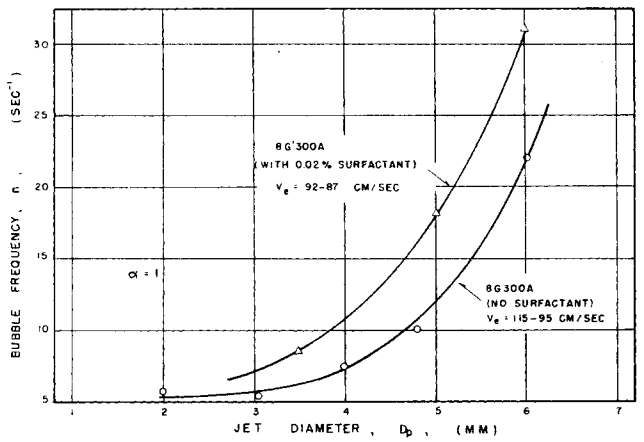

Fig. 11. Effect of surfactant on bubble frequency (at minimum entrainment velocities).

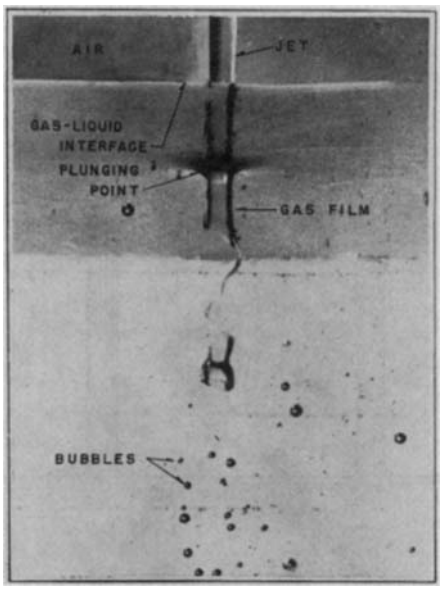

Fig. 13. Breakup of a gas film.

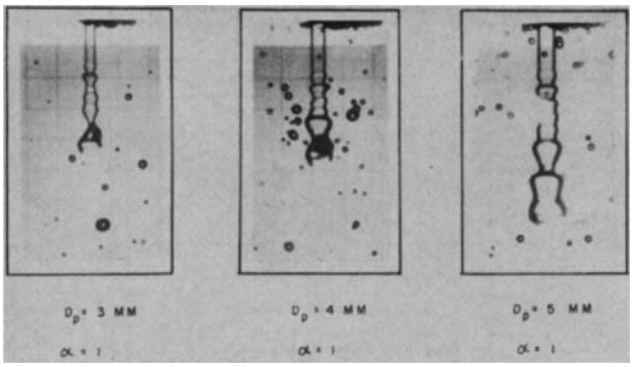

Fig. 14. Other typical gas film oscillations. System 8M130A.

observed in any of the runs at Reynolds number above 2,000. In fact, as Reynolds number exceeded about 1,500, the photographs showed that the jet became unstable in the gas phase, and disturbances developed on the jet surface. It was observed from the high-speed motion pictures that, when the extent of such disturbances was relatively small, air was entrained at the time one of the axially symmetrical waves hit the surface of the receiving liquid. This is illustrated in Figure 15(*A*). At very high Reynolds number, however, the jet surface was no longer smooth, but became ill-defined. Air seemed to be mixed into the jet stream, and bubble formation was vigorous at the plunging point. Figure 15(*B*) illustrates such a turbulent entrainment process.

It seems certain, then, that the formation of bubbles by laminar jets is the result of an enveloping air film, which breaks up due to the instability of the jet in the *liquid;* the entrainment at high Reynolds number, however, is caused by the instability of the jet in the *air,* as shown in Figure 16.

CONCLUSIONS

This research represents the only thorough investigation of the variables involved in air entrainment by vertical jets of Newtonian liquids in laminar flow as they plunge into a quiescent pool of the same liquid. It has been established that for such systems a minimum velocity is required at the plunging point to entrain air into the

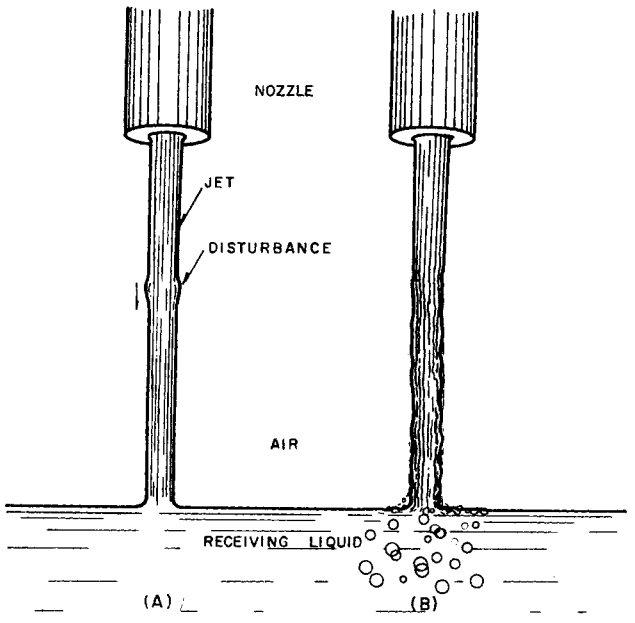

Fig. 15. Air entrainment at high Reynolds numbers.

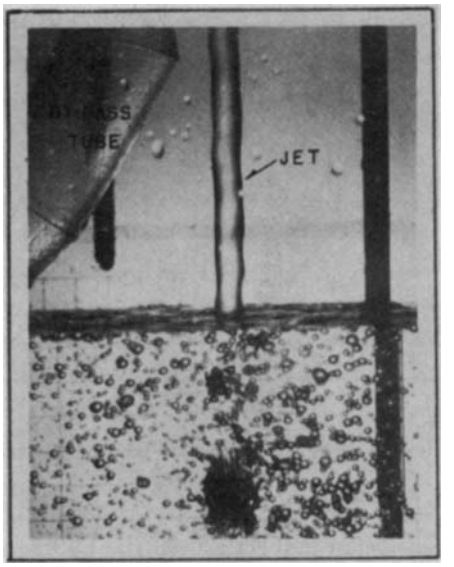

Fig. 16. Air entrainment at high Reynolds number. System 8H$_2$OA. Reynolds number at nozzle tip = 18,000.

liquid, and this velocity is a function of the density, viscosity, and surface tension of the liquid, and of the diameter of the jet at the plunging point. At minimum entrainment conditions, for laminar jets having sufficient distance in which the velocity profile can become completely relaxed before impinging on the liquid surface, the Weber number of the system is directly proportional to the three-fourths power of the Reynolds number—both being evaluated at the plunging point.

The research has also demonstrated that entirely different mechanisms govern entrainment of air by laminar and by turbulent jets of Newtonian liquids.

ACKNOWLEDGMENT

This paper presents a portion of the dissertation submitted by Tong Joe Lin to the Graduate Division of Wayne State University in partial fulfillment of the requirements for the Doctor of Philosophy degree.

NOTATION

A = abbreviation for air in experimental code
$\overline{b}$ = average bubble diameter, mm.
C = abbreviation for carbon dioxide in experimental code
D = jet diameter, mm.
D_p = jet diameter at plunging point, mm.
G = abbreviation for glycerol solution in experimental code
G' = abbreviation for glycerol solution containing 0.02% surfactant in experimental code
G'' = abbreviation for glycerol solution containing 0.2% surfactant in experimental code
G''' = abbreviation for glycerol solution containing 0.3% surfactant in experimental code
L_f = film length, mm.
M = abbreviation for mineral oil in experimental code
N_{Re_p} = Reynolds number at plunging point
N_{We_p} = Weber number at plunging point
n = bubble frequency, reciprocal sec.
P = rate of air entrainment, cc./sec.
Q = jet flow rate, cc./sec.
Q_e = jet flow rate at minimum entrainment velocity, cc./sec.
$\overline{V}$ = average jet velocity over the cross section, cm./sec.

V_e = minimum entrainment velocity (determined at the plunging point), cm./sec.
V_s = surface velocity of jet, cm./sec.
Z = jet length, cm.

Greek Letters

α = entrainment velocity ratio
γ = surface tension of liquid, dyne/cm.
μ = liquid viscosity, centipoise
ρ = liquid density, g./cc.

LITERATURE CITED

1. Birkhoff, G., and E. H. Zarantonello, "Jets, Wakes and Cavities," Academic Press, New York (1957).
2. Flack, J. E., J. I. Kveisengen, and J. H. Nath, *Science*, **134**, 392 (1961).
3. Hickox, G. H., *Civil Eng.*, **15**, 562 (1945).
4. Lane, E. W., *ibid.*, **9**, 88 (1939).
5. Straub, L. G., and A. G. Anderson, *Proc. Am. Soc. Civil Engs., Hydraulic Div.*, Paper 1890 (1958).
6. Straub, L. G., and O. P. Lamp, *Trans. Am. Soc. Civil Engs.*, **121**, 30 (1956).
7. Shirley, R. W., M.S. thesis, Univ. Iowa, Ames (1950).
8. Ohyama, Y., Y. Takashima, and H. Idemura, *Rept. Sci. Res. Inst. (Japan)*, **29**, 344 (1954).
9. Braun, I., and M. Reiner, *Quart. J. Mech. Appl. Math.*, **5**, 42 (1952).
10. Middleman, Stanley, D. Eng. dissertation, John Hopkins Univ., Baltimore (1961).
11. Philippoff, W., *Trans. Soc. Rheol.*, **1**, 95 (1957).
12. Lin, Tong Joe, Ph.D. dissertation, Wayne State Univ., Detroit (1963); Univ. Microfilms, No. 64-9539, Ann Arbor, Mich.
13. Hansen, R. S., M. E. Purchase, T. C. Wallace, and R. W. Woody, *J. Phys. Chem.*, **62**, 210 (1958).
14. Christiansen, R. M., and A. N. Hixson, *Ind. Eng. Chem.*, **49**, 1017 (1957).

Manuscript received April 14, 1965; revision received December 13, 1965; paper accepted December 15, 1965. Paper presented at A.I.Ch.E. Philadelphia meeting

Bubble Growth by Dissolution: Influence of Contact Angle

W. M. BUEHL and J. W. WESTWATER

University of Illinois, Urbana, Illinois

The rate of growth of bubbles forming on a wall from a liquid initially uniformly supersaturated with a dissolved gas was investigated. Attention was directed to the effect of the contact angle.

Theoretical predictions for the growth rate of a spherical bubble tangent to a wall were carried out with a digital computer. The predictions included the diffusion equation and the continuity equation. The energy equation was neglected; viscosity and surface tension were assumed nil. The results are compared with existing predictions for a 90-deg. contact angle. For extremely slow growth, the theoretical growth coefficient is about 30% smaller for a bubble with zero contact angle compared to one with a 90-deg. contact angle. For fast growth the difference is much less.

Experimental growth rates were determined photographically for bubbles of carbon dioxide coming out of solution from water at an artifical nucleation site. Different contact angles from 15 to 89 deg. were obtained by coating the wall with various nonwetting agents. Every bubble showed changes in its contact angle during growth. No effect of contact angle on the growth rate could be detected.

In recent years there has been much interest in the growth of bubbles in liquids, particularly in connection with the problems of heat transfer during boiling. Theoretical predictions have been given by Bosnjakovic (*1*), Epstein and Plesset (*2*), Forster and Zuber (*3*), Plesset and Zwick (*4*), Griffith (*5*), Bankoff and Mikesell (*6, 7*), Birkhoff, Margulies, and Horning (*8*), Scriven (*9*), Bruijn (*10*), Forster (*11*), Skinner and Bankoff (*12, 13*), Yang and Clark (*14*), Han and Griffith (*15*), and others. Experimental measurements have been published by Fritz and Ende (*16*), Dergarabedian (*17*), Manley (*18*), Doremus (*19*), Strenge, Orell, and Westwater (*20*), Westwater and Westerheide (*21*), Van Wijk and Van Stralen (*22*), Houghton, Ritchie, and Thomson (*23*), Benjamin and Westwater (*24*), Patten (*25*), Glas and Westwater (*26*), and others. In many respects the actual conditions existing in a liquid (particularly a boiling liquid) are not the same as those assumed by the theoretical workers. A more lengthy discussion of this is given elsewhere (*27, 28*). The exact conditions existing in a practical system are so complex that a complete analytical solution probably never will be obtained.

To bridge the gap between theory and experiment, it is necessary to determine which of the differences between real and ideal conditions are important and which are trivial. One of the common assumptions used in theoretical works is that growing or collapsing bubbles are spheres in an infinite body of liquid. An equivalent assumption used frequently (*5, 11*) is that the bubbles are hemispheres in contact with a frictionless plane in a semi-

W. M. Buehl is with Corning Glass Works, Corning, New York.